Available online at www.sciencedirect.com

ScienceDirect

Proceedings of the Combustion Institute 36 (2017) 1403–1409

Proceedings of the Combustion Institute

www.elsevier.com/locate/proci

Effects of mixture fraction on edge-flame propagation speeds

Hang Song[*], Philip Wang, Richard S. Boles, David Matinyan, Hatsachai Prahanphap, Jesse Piotrowicz, Paul D. Ronney

Department of Aerospace and Mechanical Engineering, University of Southern California, Los Angeles, CA 90089-1453, USA

Received 4 December 2015; accepted 9 July 2016
Available online 13 October 2016

Abstract

The propagation speeds (U_{edge}) of nonpremixed edge-flames were measured as a function of stoichiometric mixture fraction (Z_{st}) and global strain rate (σ) for several fuel/oxidant/diluent combinations using a counterflow slot-jet burner. It was found that for fuel Lewis number (Le_f) $\approx$ 1 and oxidant Lewis number (Le_o) $\approx$ 1 with fixed σ, U_{edge} increases monotonically with increasing Z_{st}. In contrast, for $Le_f > 1$ and $Le_o \approx 1$ with fixed σ, U_{edge} exhibits a minimum, typically at $Z_{st} \approx 0.3$, except for dimethyl ether which showed U_{edge} montonically decreasing with increasing Z_{st}. These results indicate that Z_{st} has both chemical and Lewis number effects on nonpremixed edge-flame speeds. For $Le_f \approx Le_o \approx 1$, chemical effects dominate over the whole range of Z_{st} whereas for $Le_f > 1$ and $Le_o \approx 1$, Lewis number effects become important at low Z_{st}. It is shown that all observed U_{edge} vs. Z_{st} trends are consistent with computed values of extinction strain rate (σ_{ext}) of these mixtures in a 1D counterflow, thus σ_{ext} serves as a simple surrogate for predicting edge-flame behavior.

Keywords: Edge-flame; Lewis number; Mixture fraction; Nonpremixed flames; Counterflow

1. Introduction

"Edge-flames" occur along the length of flame sheets where transitions from burning to non-burning conditions exist. Edge-flame behavior is used to interpret many types of non-uniform flame phenomena including flames in highly turbulent flows such as reciprocating-piston internal combustion engines where "holes" in flame sheets may open or re-seal, flames stabilized near a cold wall or splitter plate, or leading edges of flames spreading across condensed-phase fuel surfaces [1]. The most important property of an edge-flame is its propagation speed (U_{edge}), defined as the speed the edge moves relative to the unburned gases in the direction parallel to the flame sheet. Previous theoretical studies of edge-flames in premixed [2–4] and nonpremixed [5–9] configurations predict that edge-flames may propagate from the burning into the non-burning region, forming an "ignition front" with $U_{edge} > 0$ or retreat into

---

[*] Corresponding author.
E-mail addresses: songhang@stanford.edu, songhang@usc.edu (H. Song).

http://dx.doi.org/10.1016/j.proci.2016.07.042
1540-7489

the burned region, forming an "extinction front" with $U_{edge} < 0$. Many factors affect U_{edge} such as global strain rate (σ), Lewis numbers (Le, ratio of mixture thermal diffusivity to reactant mass diffusivity) of fuel and oxidant, heat losses, and for nonpremixed edge-flames the stoichiometric mixture fraction $Z_{st} \equiv 1/(1 + \nu X_f/X_o)$ where ν is the stoichiometric oxygen-to-fuel mass ratio and X_f and X_o are the mass fractions of fuel and oxygen in the unburned mixture streams.

While traditional nonpremixed combustion generally employs pure hydrocarbons mixing and burning with highly-diluted oxygen (specifically, air) resulting in low Z_{st} (typically 0.06), new fuels and combustion technologies (biofuels, oxyfuel combustion, massive exhaust gas recirculation, etc.) result much broader Z_{st} ranges – up to 0.8 for pure oxygen burning with highly-diluted fuel. In the widely-employed counterflow geometry, increasing Z_{st} moves the flame location from the oxidizer side toward the fuel side of the stagnation plane, which results in significant differences in the reactant temperature/composition/time history. This was shown [10,11] to cause very asymmetric flame properties with respect to $Z_{st} = 0.5$ (where the flame resides at the stagnation plane) which was attributed [11] to shifts in O_2 concentration profiles as Z_{st} increases to coincide more closely with peak temperature locations, leading to increased radical production rates and thus more robust flames. No theoretical or computational study has examined Z_{st} effects on edge-flame properties. Prior nonpremixed edge-flame experiments [10] focused primarily on $Z_{st} = 0.5$ with one data set taken at $Z_{st} = 0.2$ and 0.8 for CH_4/N_2–O_2/N_2 mixtures for which Lewis numbers of fuel (Le_f) and oxygen (Le_o) are near unity. Studies of Le effects are relevant to systems employing fuels with very high or low molecular masses, resulting in widely varying Le_f which strongly affects U_{edge} and extinction behavior [10] and, as will be shown, couple with Z_{st} effects in unusual ways.

Accordingly, this work's objective is to study systematically Z_{st} effects on edge-flame properties for varying σ and varying Lewis numbers (by varying fuel and diluent type). Following prior work [10] a counterflow slot-jet (rather than round-jet) apparatus is employed because slot-jets provide extensional strain orthogonal to the slot plane yet little convection along the slot length, thus edge-flame propagation speeds in the laboratory frame are the propagation speed relative to the cold unburned gas far ahead of the edge-flame (or behind, for retreating edge-flames). This approach simplifies interpretation of experimental data.

2. Experimental apparatus, procedures, scaling

The counterflow slot-jet apparatus and procedures are similar those employed previously [10]. Thermal mass flow controllers regulated fuel and oxidizer jet exit velocities (U_f, U_o) to obtain specified $\sigma = (U_o + U_f)/d$ (d = jet spacing, typically 7.5 mm) and mixtures (fuel+diluent and O_2 +diluent) at the required X_o and X_f to obtain specified Z_{st}. Honeycomb inserts at the jet exits provided uniform flow across the jets' width (5 mm) and length (130 mm). Nitrogen sheath flows with the same exit velocities as the reactive jets were employed on both sides of both reactant streams to prevent secondary flames. The jets were maintained at room temperature by water-cooling. The apparatus was enclosed in a ventilated box to suppress room draft influences. A schematic and photograph of the apparatus are given in Figure S1. Edge-flame propagation or retreat was recorded using high-speed video.

For conditions resulting in $U_{edge} > 0$, an N_2 jet was used to extinguish or "erase" the flame starting at one end, then the jet was retracted, enabling the edge-flame to advance. For conditions resulting in $U_{edge} < 0$, first a mixture having $U_{edge} > 0$ was introduced, then electrically-heated wires at both slot ends were activated, then X_o and X_f were slowly reduced to the desired values. The heated wires provided localized flame temperature enhancement, thus locally increased reaction rates at the flame ends, anchoring these ends under conditions where they would retreat without localized heating. To induce extinction, the N_2 jet was introduced to separating one flame end from its anchoring hot-wire, enabling observation of the retreating edge-flame. Video data were analyzed to infer U_{edge}. Because the slot-jet aspect ratio is finite there is a slight extensional flow along the slot length which slightly affects U_{edge} in the laboratory frame; as in prior work [10], this bias is nullified by interpolating U_{edge} vs. position along the slot to the jet centerline.

Table 1 shows the mixtures employed. The "baseline" case was CH_4–N_2 vs. O_2–N_2 which provides $Le_f \approx Le_o \approx 1$. All CH_4–N_2/O_2–N_2 compositions were created so that stoichiometric combinations of fuel and oxidant streams result in $CH_4/O_2/N_2 = 1/2/9.5$ (increasing Z_{st} corresponds to more of the 9.5 N_2 from the O_2 to CH_4 stream), thus all stoichiometric combinations have the same premixed-flame properties, specifically unburned-to-burned gas density ratio (ρ_u/ρ_b), adiabatic flame temperature (T_f) and laminar burning velocity (S_L). CH_4–CO_2 vs. O_2–CO_2 mixtures were chosen to provide $Le_f \approx Le_o < 1$. C_4H_{10}–N_2 vs. O_2–N_2 mixtures were chosen to have nearly the same S_L as the CH_4–N_2 vs. O_2–N_2 mixtures with $Le_o \approx 1$ again but now $Le_f > 1$. Both n-C_4H_{10} and i-C_4H_{10} were tested to assess possible effects of low-temperature chemistry, since n-C_4H_{10} decomposes more readily at low temperatures and thus has shorter ignition delays [12,13]. C_4H_{10}–CO_2 vs. O_2–CO_2 mixtures were chosen to provide reactant Lewis numbers "straddling" unity ($Le_f > 1$ but $Le_o < 1$).

Table 1
Properties of the mixtures tested. S_L was calculated using CHEMKIN [15] with USC Mech II kinetics [16], except for CH_3OCH_3 where [17] was used.

Fuel	Diluent	Fuel/O_2/Diluent	Le_f	Le_o	ρ_u/ρ_b	T_f	S_L (cm/s)
CH_4	N_2	1 / 2 / 9.5	0.96	1.10	6.81	2024	21.3
CH_4	CO_2	1 / 2 / 7	0.73	0.83	6.15	1828	5.19
iso-C_4H_{10}	N_2	1 / 6.5 / 30	2.16	1.04	7.37	2100	20.4
n-C_4H_{10}	N_2	1 / 6.5 / 30	2.16	1.04	7.40	2109	26.7
iso-C_4H_{10}	CO_2	1 / 6.5 / 20	1.73	0.77	7.06	1980	7.29
n-C_4H_{10}	CO_2	1 / 6.5 / 20	1.73	0.77	7.09	1987	11.0
C_3H_8	N_2	1 / 5 / 24.6	1.86	1.05	7.10	2040	22.1
CH_3OCH_3	N_2	1 / 3 / 17	1.81	1.02	6.87	1948	22.1

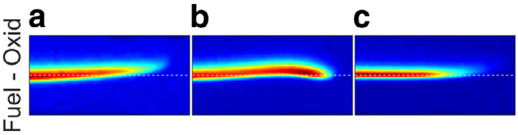

Fig. 1. False-color images of direct emission from edge-flames in mixtures of i-$C_4H_{10}/O_2/CO_2 = 1/5/20$, $Z_{st} = 0.5$: (a) $\sigma = 14$/s, retreating from right to left; (b) $\sigma = 20$/s, advancing from left to right; (c) $\sigma = 43$/s, retreating from right to left.

Finally C_3H_8–N_2 vs. O_2–N_2 and CH_3OCH_3–N_2 vs. O_2–N_2 mixtures with nearly the same S_L as the other fuel-O_2–N_2 mixtures were compared since C_3H_8 and CH_3OCH_3 (dimethyl ether, DME) have nearly the same Le_f but DME has much greater low-temperature reactivity since (unlike most hydrocarbons) DME does not inhibit its own oxidation; this is because the inhibiting reaction of oxygen with the fuel radical obtained from H atom abstraction cannot occur with DME [14].

Edge-flame theory [5–8] predicts that for adiabatic edge-flames with $Le_f = Le_o = 1$, constant density and low σ, $U_{edge}/S_L = 1$. Moreover, effects of density variation on U_{edge} scales with $(\rho_u/\rho_b)^{1/2}$ [18]. Consequently, we expect $U_{edge}/S_L(\rho_u/\rho_b)^{1/2} \approx 1$ if Lewis number and heat loss influences are negligible, thus all U_{edge} data are scaled accordingly.

3. Results and discussion

3.1. Experiments

Figure 1 shows false-color direct images of typical edge-flames. In all cases the trailing regions are essentially flat and showed traditional nonpremixed flame behavior. Fast-advancing edge-flames generally show some curvature near the leading edge (Fig. 1b) whereas retreating (Fig. 1a and c) and slowly advancing edges are generally nearly flat.

Figure 2a–h show the effects of Z_{st} on the scaled edge-flame speed for each fuel/O_2/diluent combination tested. Results are plotted for several fixed values of global strain rate σ so the effect of Z_{st} with all other experimental parameters held constant is readily seen. It should be noted that for each of these eight plots, on each plot, every point corresponds to the same mixture (same ratio of fuel/O_2/diluent, thus same ρ_u/ρ_b, T_f and S_L) when fuel and O_2 streams are combined in stoichiometric proportions, yet the resulting behavior varies drastically depending on Z_{st} and σ.

For the baseline CH_4–N_2 vs. O_2–N_2 mixtures (Fig. 2a), several features are apparent. First, U_{edge} increases monotonically with Z_{st} for all strain rates (σ), rather than being symmetric with respect to $Z_{st} = 0.5$. This is consistent with limited prior edge-flame data [10] as well as the effect of Z_{st} on extinction strain rate (σ_{ext}) of uniform nonpremixed counterflow flames [11]. The reasons for this chemical effect were discussed in Section 1; a key question addressed in this work is whether this trend is universal. Second, as is well known from theory [8] and prior experiments [10], extinction limits ($U_{edge} \rightarrow -\infty$) exist at both high and low σ, due to insufficient residence time and heat losses, respectively. Third, even for fixed σ, U_{edge} can actually transition from positive to negative values to extinction as Z_{st} is decreased. Fourth, for intermediate σ (about 20/s - 50/s, away from both low-σ and high-σ extinction limits) there is almost no effect of σ on U_{edge}. Finally, the scaled non-dimensional edge-flame speeds are significantly less than/greater than unity for small/large values of Z_{st}, indicating unexpectedly weak/strong flames depending on Z_{st}.

The reported values of σ may appear rather low, however, it should be noted that these are global strain rates based on cold-flow properties; the axial velocity gradient $\partial u/\partial x$ at the reaction zone are much larger due to thermal expansion effects. Computations (described below) show that, for example, for CH_4–N_2 vs. O_2–N_2 mixtures with $Z_{st} = 0.5$ and global $\sigma = 96$/s, $\partial u/\partial x$ at $Z = Z_{st}$ is 424/s. Nevertheless, global properties are considered relevant because $\partial u/\partial x$ varies both in the streamwise and spanwise direction near the flame edge, thus no uniquely-definable local value of σ exists for edge-flames. Moreover, correlations of strain effects on turbulent flames [19] typically employ global strain rate estimates based on the cold-flow conditions.

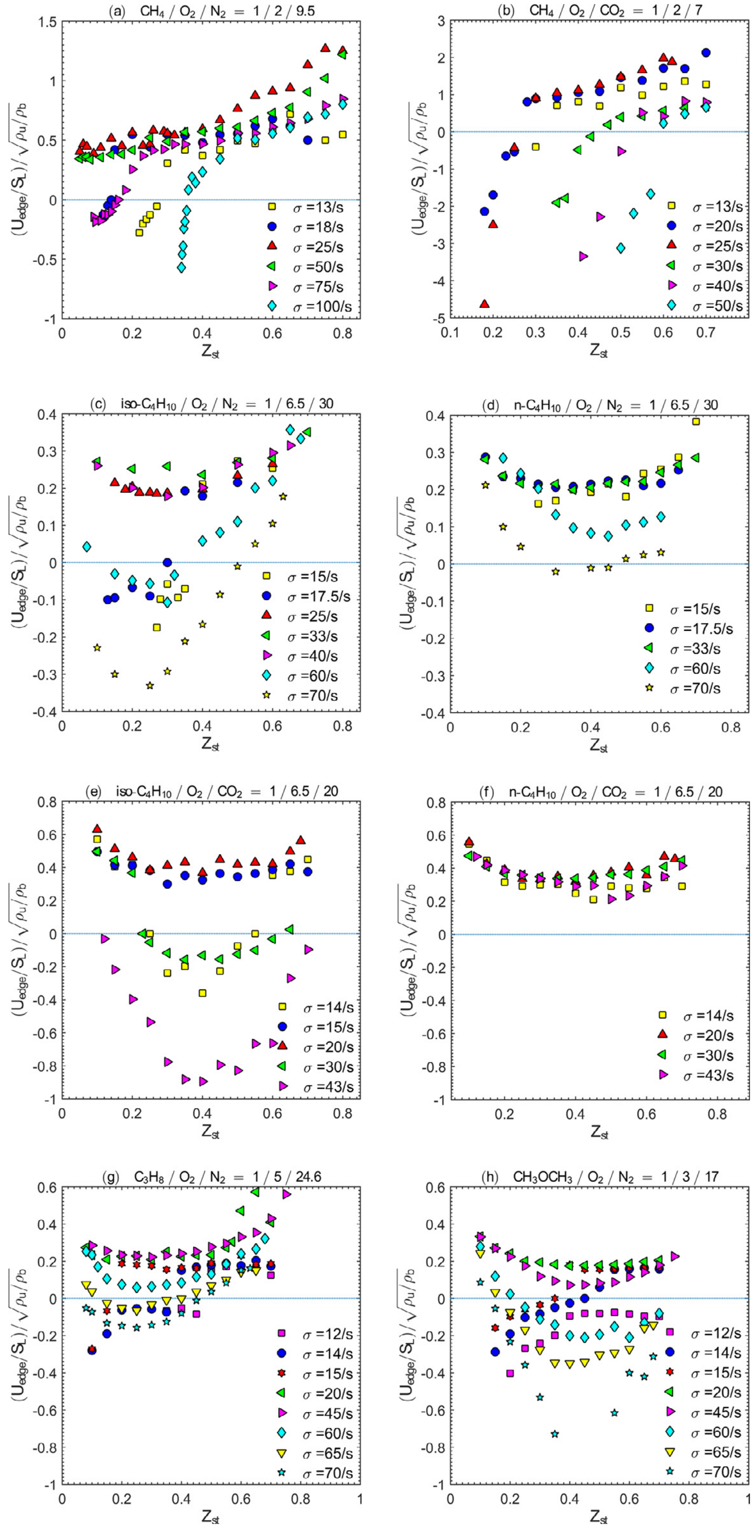

Fig. 2. Effect of Z_{st} on scaled edge-flame speeds for several fixed values of global strain rate σ.

Figure 2b shows that mixtures with $Le_f \approx Le_o < 1$ show the same trends observed for the baseline $Le_f \approx Le_o \approx 1$ case, namely that U_{edge} increases monotonically with increasing Z_{st}, i.e. the same chemical effect exists. The only substantive difference is that away from extinction limits the scaled non-dimensional edge-flame speeds can be much greater than in the $Le_f \approx Le_o \approx 1$ case; it is well established both theoretically [9] and experimentally [10] that U_{edge} increases substantially with decreasing Le.

Figure 2c shows that a larger hydrocarbon (i-C_4H_{10}) having $Le_f > 1$ (but still employing O_2–N_2 oxidizer so that $Le_o \approx 1$) exhibits drastically different behavior, specifically U_{edge} vs. Z_{st} is non-monotonic (U-shaped) with the lowest values at $Z_{st} \approx 0.3$; in fact, for some σ, U_{edge} is positive at high and low Z_{st} yet negative at intermediate Z_{st}. Seemingly the same chemical effect found for CH_4 is present at high Z_{st} but some additional factor affects U_{edge} at low Z_{st}. All scaled values of U_{edge} are much less than unity because of high Le_f. Again, both high- and low-σ extinction limits exist.

To search for the cause of this unusual non-monotonic behavior, U_{edge} was measured for n-C_4H_{10} fuel (Fig. 2d) under conditions otherwise identical to i-C_4H_{10} (Fig. 2c). This strategy assesses the effect of fuel structure, specifically low-temperature chemistry which is more prevalent in n-C_4H_{10}. Figure 2d shows that non-monotonic behavior is also observed with n-C_4H_{10}. Away from low-σ and high-σ extinction limits, U_{edge} is nearly identical for i-C_4H_{10} and n-C_4H_{10}, however, close to both limits n-C_4H_{10} has much higher U_{edge}. Consequently, low-temperature chemistry apparently affects U_{edge} near extinction limits, but is not the root cause of the non-monotonic trend.

To assess the relative roles of Le_f and Le_o, U_{edge} was measured for i-C_4H_{10}–CO_2 and n-C_4H_{10}–CO_2 vs. O_2–CO_2 mixtures (Fig. 2e and f) for which Le_f and Le_o "straddle" unity. No significant qualitative difference from the comparison of i-C_4H_{10}–N_2 and n-C_4H_{10}–N_2 vs. O_2–N_2 mixtures was observed, although again scaled non-dimensional values of U_{edge} are much larger with CO_2 dilution because of the lower Lewis numbers. For both CH_4 and C_4H_{10} fuels, CO_2-diluted mixtures have scaled non-dimensional values of U_{edge} that are roughly twice that of N_2-diluted mixtures.

One possible explanation for the non-monotonic behavior of U_{edge} is as follows. It is well known [20] that for strained counterflow flames near extinction with single-step chemistry, the more fully consumed reactant (that does not leak significantly through the reaction zone) is O_2 for $Z_{st} < 0.5$ and fuel for O_2 for $Z_{st} > 0.5$. Prior work on diffusive-thermal instabilities of nonpremixed flames [21] showed that the effective Lewis number (for interpreting instability behavior) is that of the more fully consumed reactant. Consequently, for sufficiently low Z_{st} the "effective" Le (Le_{eff}) should be Le_o whereas for high Z_{st} it should be Le_f. If $Le_f \approx Le_o$ then Le_{eff} would be the same for all Z_{st} and only the chemical effect (which causes U_{edge} to increase monotonically with Z_{st}) would be present. However, for cases with $Le_f > Le_o$, Le_{eff} would be lower ($\approx Le_o$) at low Z_{st} and higher ($\approx Le_f$) at high Z_{st}. The lower Le_{eff} at low Z_{st} would in turn lead to higher U_{edge} than if Le_{eff} were constant. This explanation of the combined chemical + Lewis number effects is entirely consistent with the observed monotonic behavior of U_{edge} for $Le_f \approx Le_o$ and U-shaped behavior for $Le_f > Le_o$, however, Seshadri and Bai [22] showed that hydrocarbon-oxygen oxidation in nonpremixed flames does not behave according to this simple single-step reaction model; in fact, O_2 is the leaking reactant for all Z_{st} because hydrocarbon decomposition by radicals is much more rapid than O_2 decomposition. Nevertheless, fuel will survive part-way to the radical production zone and thus Le_f may be expected to have some effect on Le_{eff} and thus U_{edge}.

To assess the effect of fuel decomposition rates, DME is appropriate because of its significant low-temperature reactivity compared to hydrocarbons (see Section 1). For comparison with hydrocarbons, propane was selected because its Le_f is very similar to DME. As might be expected, C_3H_8–N_2 vs. O_2–N_2 mixtures (Fig. 2g) show behavior very similar to i-C_4H_{10}–N_2 vs. O_2–N_2 mixtures (Fig. 2c) but with slightly higher values of U_{edge} due to the slightly lower Le_f of C_3H_8. In contrast, CH_3OCH_3–N_2 vs. O_2–N_2 mixtures (Fig. 2h) show higher values of U_{edge} than C_3H_8–N_2 vs. O_2–N_2 mixtures (Fig. 2g) at low Z_{st} but lower values of U_{edge} at high Z_{st}.

3.2. *Computations*

In order to interpret these data, rather than attempting brute-force calculations of multidimensional edge-flames, we attempted to identify (if possible) an easily-determined 1D flame parameter characterizing the effects of Z_{st}. The premixed laminar burning velocity (S_L) of the stoichiometric mixture of fuel and oxidant streams is clearly inappropriate since for each plot (Fig. 2a–h), S_L is the same for every point. In contrast, the adiabatic extinction strain rate (σ_{ext}) is known [11] to depend on Z_{st} in a manner similar to the observed effect of Z_{st} on U_{edge}, at least for CH_4–N_2 vs. O_2–N_2 mixtures. With this motivation σ_{ext} vs. Z_{st} in a 1D counterflow was computed for all mixtures studied experimentally, using the same jet exit velocities and jet spacings as the experiments. Figure 3 shows the computed (using the same code and kinetic data used to obtain S_L in Table 1) effect of Z_{st} on the high-σ extinction strain rate (σ_{ext}) Qualitatively, computed values of σ_{ext} show trends with Z_{st} remarkably similar to the measured effects of Z_{st} on U_{edge} for σ not close to either the high-σ or low-σ extinction limits. Specifically both the experimental U_{edge} and

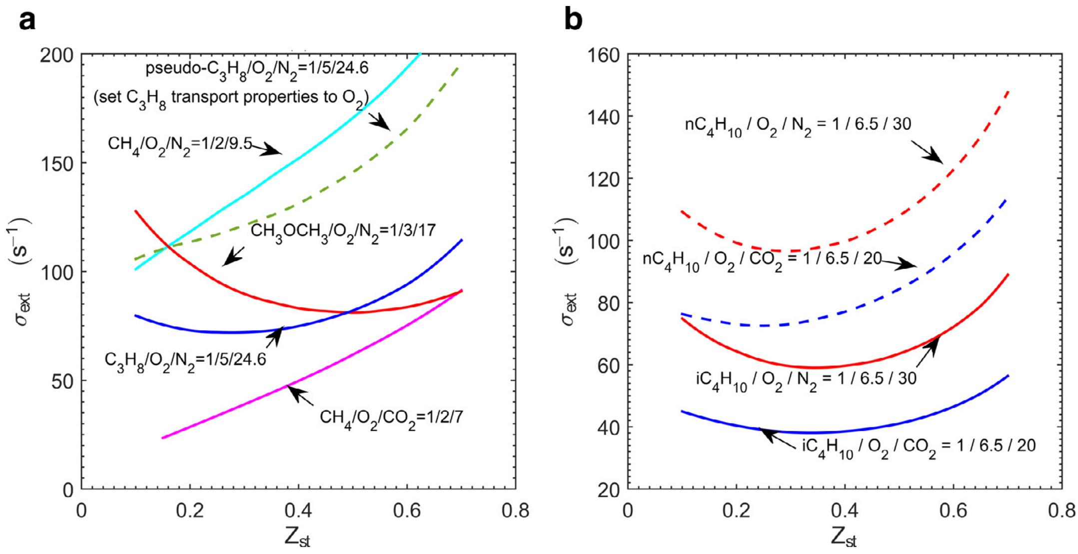

Fig. 3. Computed effect of Z_{st} on extinction strain rates in 1D counterflows for all mixtures tested (Table 1). (a) CH_4, C_3H_8 and CH_3OCH_3 mixtures; (b) n-C_4H_{10} and i-C_4H_{10} mixtures.

Table 2
Comparisons of measured and computed extinction strain rates (units s^{-1}).

Mixture	Z_{st}	σ_{ext} (exp)	σ_{ext} (comp)
$CH_4/O_2/N_2$	0.08	75	98
	0.32	100	137
$CH_4/O_2/CO_2$	0.18	25	27
	0.40	40	49
	0.50	50	61
i-$C_4H_{10}/O_2/N_2$	0.20	70	64
i-$C_4H_{10}/O_2/CO_2$	0.40	45	38
$C_3H_8/O_2/N_2$	0.25	75	71
$CH_3OCH_3/O_2/N_2$	0.35	70	85
	0.55	70	80

computed σ_{ext}: (1) increase monotonically with Z_{st} for CH_4–O_2-diluent mixtures; (2) exhibit U-shaped trends with minima at $Z_{st}\approx$0.3-0.4 for all C_3H_8 and C_4H_{10} cases; (3) are higher for all n-C_4H_{10} than i-C_4H_{10} cases; and (4) are higher for CH_3OCH_3 than C_3H_8 at low Z_{st} with the opposite behavior at high Z_{st}. Table 2 shows quantitative comparisons of σ_{ext} inferred from experimental data (where $U_{edge}\rightarrow-\infty$) to predictions (Fig. 3). The ratio of experimental to computed values of σ_{ext} are on average 0.91 with a standard deviation of 0.15. No adjustments to either model or experiment were made to obtain this agreement. These qualitative and quantitative comparisons strongly suggest that σ_{ext} is a suitable 1D property for interpreting the behavior of multi-dimensional edge-flame structures.

With this motivation, numerical experiments were performed in which the reactant transport properties were modified from their real values to assess Lewis number effects. Figure 3a shows that for C_3H_8–O_2–N_2 mixtures, artificially setting the Lennard–Jones parameters of C_3H_8 equal to those of O_2 (effectively forcing $Le_f\approx Le_o\approx 1$ as with CH_4–O_2–N_2 mixtures) caused σ_{ext} values (dashed curve) to become monotonic with Z_{st} and quantitatively very similar to CH_4–O_2–N_2 mixtures. Consequently, the non-monotonic (U-shaped) behavior of U_{edge} vs. Z_{st} for the higher hydrocarbons is very likely a result of Lewis number rather than chemical effects, whereas the unusual behavior of DME at low Z_{st} is clearly related to the contrasting (compared to hydrocarbons) behavior of its well-known [14] low-temperature chemistry.

4. Conclusions

This work investigated the effect of stoichiometric mixture fraction (Z_{st}) on the propagation speeds of nonpremixed edge-flames (U_{edge}) in a variety of strategically-chosen hydrocarbon-diluent vs. O_2-diluent combinations, with the intent of examining systematically the effects of transport and chemical effects, specifically Lewis numbers and high-temperature vs. low-temperature chemistry. Interpretation of results was facilitated by the use of values of fuel and oxidizer mass fractions such that, for a given fuel and diluent type, all stoichiometric combinations of the fuel and oxidizer streams result in the same mixture (thus same adiabatic flame temperature, density ratio and premixed laminar burning velocity) even though

Z_{st} varies widely depending on how the diluent is distributed between these streams.

With this approach to varying Z_{st} it could be expected that U_{edge} would be constant since all values of Z_{st} result in the same fuel:O_2:diluent mixture, but clearly U_{edge} is far from constant as Z_{st} is varied. At the second level, it could be expected that U_{edge} would be symmetric with respect to $Z_{st} = 0.5$, but again this is not the case even when fuel and oxidant have similar Lewis numbers, due to the previously-documented asymmetry of fuel vs. O_2 decomposition in counterflow nonpremixed flames [11]. At the third level, it could be expected that U_{edge} would be the same for fuels with similar Le, but even this is not the case due to low-temperature chemistry effects (propane vs. DME, n-butane vs. iso-butane). As a result of the interactions of Lewis number and chemistry effects, U_{edge} may increase or decrease with increasing Z_{st}, or have a non-monotonic (U-shaped) behavior. Despite these potentially complicated interactions, it was found that all observed U_{edge} vs. Z_{st} trends are consistent with computed values of extinction strain rate (σ_{ext}) of these mixtures in a 1D counterflow, thus σ_{ext} serves as a simple surrogate for predicting edge-flame behavior.

These results indicate that the behavior of highly turbulent nonpremixed flames near extinction (where edge-flames develop [23]) depends critically on (1) fuel type (through Lewis number and chemical effects), (2) degree of dilution of both fuel and oxidizer (characterized by Z_{st}), and (3) strain rate. This work provides some insight on the combined effects of these factors.

Acknowledgments

The authors are grateful to Prof. K. Seshadri for helpful discussions. This work was supported by the U.S. National Science Foundation, grant CBET-1236892.

Supplementary materials

Supplementary material associated with this article can be found, in the online version, at doi:10.1016/j.proci.2016.07.042.

References

[1] F.A. Williams, *Combustion Theory*, 2 Ed., Westview Press, Boulder, CO, 1985.
[2] J.D. Buckmaster, *Prog. Energy Combust. Sci.* 28 (2002) 435–475.
[3] T.G. Vedarajan, J.D. Buckmaster, *Combust. Flame* 114 (1998) 267–273.
[4] T.G. Vedarajan, J.D. Buckmaster, P.D. Ronney, *Proc. Combust. Inst.* 27 (1998) 537–544.
[5] J. Daou, A. Liñán, *Combust. Flame* 118 (1999) 479–488.
[6] J.D. Buckmaster, *Combust. Sci. Technol.* 115 (1996) 41–68.
[7] J. Daou, A. Liñán, *Combust. Theory Model.* 2 (1998) 449–477.
[8] R. Daou, J. Daou, J. Dold, *Proc. Combust. Inst.* 29 (2002) 1559–1564.
[9] R. Daou, J. Daou, J. Dold, *Combust. Theory Model.* 8 (2004) 683–699.
[10] M.S. Cha, P.D. Ronney, *Combust. Flame* 146 (2006) 312–328.
[11] R. Chen, R.L. Axelbaum, *Combust. Flame* 142 (2005) 62–71.
[12] S. Gersen, A.V. Mokhov, J.H. Darmeveil, H.B. Levinsky, *Combust. Flame* 157 (2010) 240–245.
[13] D. Healy, N.S. Donato, C.J. Aul, et al., *Combust. Flame* 157 (2010) 1540–1551.
[14] A. Rodriguez, O. Frottier, O. Herbinet, et al., *J. Phys. Chem. A* 119 (2015) 7905–7923.
[15] CHEMKIN 15131, *Reaction Design*, 2013 San Diego.
[16] H. Wang, X. You, A.V. Joshi, et al., *USC Mech Version II*, 2007 http://ignis.usc.edu/USC_Mech_II.htm.
[17] S.L. Fischer, F.L. Dryer, H.J. Curran, *Int. J. Chem. Kinet.* 32 (2000) 713–740.
[18] R. Ruetsch, L. Vervisch, A. Liñán, *Phys. Fluids* 7 (1995) 1447–1454.
[19] D. Bradley, *Proc. Combust. Inst.* 24 (1992) 247–262.
[20] A. Liñán, *Acta Astronaut* 1 (1974) 1007–1039.
[21] R.H. Chen, G.B. Mitchell, P.D. Ronney, *Proc. Combust. Inst.* 24 (1992) 213–221.
[22] K. Seshadri, X.S. Bai, *Proc. Combust. Inst.* 31 (2007) 1181–1188.
[23] A. Bhagatwala, E.R. Hawkes, J.H. Chen, in: 9th U.S. National Combustion Meeting, Cincinnati, OH, May 2015.